PROBABILISTIC PERFORMANCE ASSESSMENT FOR MASONRY STRUCTURES OF SCHOOL BUILDINGS IN EL SALVADOR

Luis Ernesto Mixco Durán*   Supervisor: Shunsuke SUGANO**
MEE17713

ABSTRACT

This study focuses in the Probabilistic Performance Assessment for Masonry Structures of School Buildings in El Salvador, through analytical fragility functions and its application to seismic risk analysis, following the Performance-based Earthquake Engineering (PBEE) methodology developed by PEER Center. Three combinations of two-story masonry buildings with openings (A: Mixed, B: Reinforced Concrete Masonry Infill and C: Confined Masonry Walls) were taken as target structures, based on configurations commonly found in the school's portfolio of the country. Updated results of a Probabilistic Seismic Hazard Assessment and soil amplification effects of El Salvador, were used. Similarly, both the variation of seismic demand response as the deformation capacities of each structure, have been taken into account. Three performance levels, known as Immediate Occupancy (IO), Life Safety (LS) and Collapse Prevention (CP) limit states, were deemed, on which the Seismic Demand and Damage Fragility Functions were built, along with the calculation of the Failure Probabilities in terms of Mean Annual Frequencies (MAFs) of each combination. Results indicate that for IO and LS limit states, the Combination B has the highest structural reliability (best seismic performance) for both intensity measures [PGA and Sa (T1, 5%)], due to its low failure probabilities obtained concerning the other combinations. For the CP limit state, the combination C provides the greater structural reliability for both intensity measures. Nevertheless, none of the combinations managed to meet the acceptable MAFs at the less frequent seismic hazard levels of 475 and 975 years of return period.

Keywords: Confined Masonry, Masonry Infill, Limit States, Fragility Function, Failure Probability.

1. INTRODUCTION

In the last two centuries, El Salvador has suffered the onslaught of earthquakes from the two main seismic sources that affect the country, shallow upper-crustal earthquakes due to geological local faults activation (1965 and 1986 events), and offshore earthquakes due to subduction processes (2001 events). These kinds of earthquakes have exposed the high seismic vulnerability of existing buildings along the country, especially those that belong to the education sector. Several types of structures are found in the school portfolio, where masonry structures are predominant, and until now very few studies exist that deal more closely with their seismic risk in an integral manner. The principal objective of this study is to perform a Probabilistic Safety Assessment of three popular configurations (combinations) of school masonry buildings focusing in three limit states associated to a shear failure mechanism and determine which of them has more reliability against different design earthquakes hazard levels. A secondary objective is to focus in the Conditional Failure Probability for specific acceleration ground motion through the derivation of Seismic Demand and Damage Fragility Curves for the three combinations and make comparison between them, considering the variation in both, the seismic demand response and deformation capacities, with a strict management of its aleatory and epistemic uncertainties.

---

* Ministry of Environment and Natural Resources, El Salvador.
**Professor Emeritus, Hiroshima University, and Visiting Research Fellow, IISEE, BRI, Japan.

2. METHODOLOGY

The methodology used in this study is based on the analytical steps of the innovative Performance-Based Earthquake Engineering (PBEE) developed by Pacific Earthquake Engineering Research (PEER) Center. Generally, this starts from the definition of the target building, the determination of the non-linear properties of its constituent structural elements and its grouping into an advanced computational model. Then the results obtained from a probabilistic seismic hazard model, at the site of interest, are used to collect ground motions that will be applied to the structure. The response of the structure to these seismic demands is obtained with a probabilistic seismic demand analysis, based on a nonlinear dynamic analysis. To assess the ability of the structure to support such seismic actions, a probabilistic seismic capacity analysis is carried out, based on reviewing real test data and comparing with empirical model reflected in the nonlinear static pushover analysis results. Finally, the seismic reliability analysis of the structure against the exceedance of limit states is obtained.
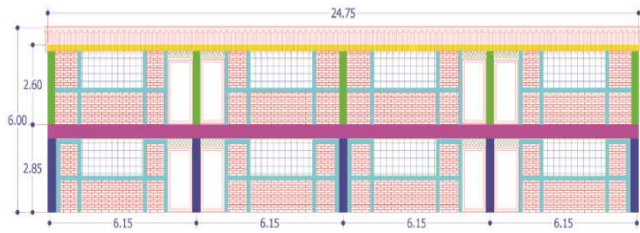
3. SELECTION OF TARGET BUILDING

Figure 1. Typical façade of the target building.

In Figure 2, a typical façade of target building in direction X is observed. This corresponds to a prototype structure commonly used for school buildings in El Salvador. Therefore, three types of systems were selected as target buildings. These are based on three combinations (named as A, B, and C) of two-story masonry buildings, where openings (windows and doors) are found in their longest direction. The combination A was defined in its 1st level of RC masonry infill (MI) walls and the 2nd story of Confined Masonry (CM) walls, the combination B has in its 1st and 2nd story RC MI walls and the combination C has in its 1st and 2nd story CM walls. During the construction of the computational model of each building, it was obtained that the eigenvalue first mode period of the combination A, B, and C, were 0.174 sec., 0.179 sec., and 0.124 sec., respectively.

4. NONLINEAR PROPERTIES OF MI AND CM WALLS

Three computational 3D models for each structural combination were built. The STERA3D V9.6 software (Saito T. 2004) was used to perform the non-linear analysis, which provides some built-in hysteresis models and represents internal stress-deformation with non-linear springs. For the MI panels, the analytical model from (Mostafaei & Kabeyasawa, 2004) was used. This model is based on a degrading trilinear backbone curve similar to that shown in Figure 3, where restoring forces and deformation capacities of Cracking (τ_{cr}, R_{cr}), Maximum (τ_{max}, R_{max}) and Ultimate (τ_u, R_u) States of the walls, comes to light. It is important to highlight, the need to use more detailed expressions that involve factors that influence the in-plane

Figure 2. Backbone curve of MI and CM walls with a Shear Failure Mode.

structural capacity of MI walls, based on experimental data instead of using an analytical approach. For this reason, during this study, Dr. Sugano was developing equations for each characteristic point using real experimental data and considering a Masonry Infill wall (RC columns + infill panel) as one element. Thus, this would give a chance (for future works) to obtain more precise values of the MI non-linear behavior. For the CM walls in the combination C, a similar shape of the backbone curve in Figure 3 was used, where the value of each characteristic point is obtained from Sugano, S. 2018 empirical equations.
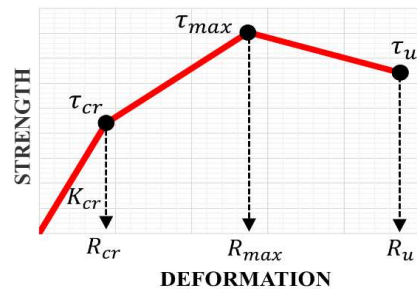
5. PROBABILISTIC SEISMIC HAZARD ASSESSMENT (PSHA)

The PSHA focuses on characterizing the seismic threat at the site where the structure is located, by estimating the MAF of exceeding a specified ground motion intensity measure (IM), either PGA or Sa (T_1, 5%). As a product of this analysis, both uniform hazard spectra (UHS) and seismic hazard curves, are obtained. Furthermore, this analysis helps to select a set of ground motions that jointly represent the site hazard through four earthquake design levels (or hazard levels): 72, 250, 475 and 975 years of return period. Figure 3 shows the approximation of seismic hazard curve for PGA and its equation in terms of MAF. This approximation was made using the acceleration values (from the PSHA) for the four hazard levels on soft soil site conditions. Figure 4 shows the response spectra of selected 40 ground motions which satisfy (as much as possible) the results from the seismic hazard disaggregation for a specific period. This figure also shows a scaling technique based on the matching of the response spectra with the UHS for a hazard level (e.g., 475 years), over a range of periods, which include the natural periods of structural combinations, to minimize the dispersion in the nonlinear dynamic response.
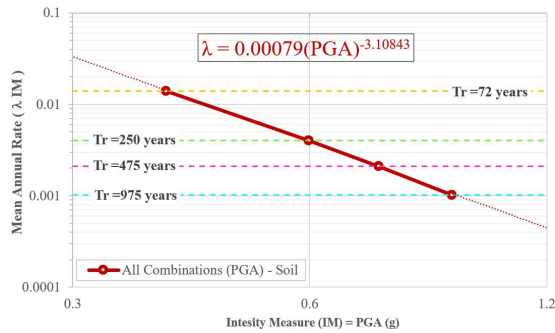

Figure 3. Linear function and its equation of seismic hazard curve for PGA and four design earthquakes levels applied for all three combinations.
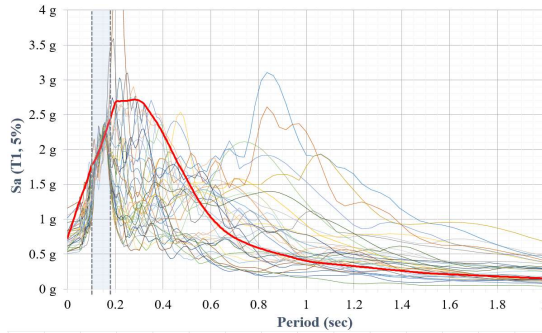

Figure 4. 40 ground motions response spectra matched to the UHS for 475 years of return period (solid red line) over a range of periods of 0.12-0.18 sec (vertical dashed lines).

6. DAMAGE AND LIMIT STATES OR PERFORMANCE LEVELS

In this study, the Maximum Interstory Drift Ratio (IDRmax) has been chosen as the engineering demand parameter (EDP) to measure the structural demand response. This measure can be related with the quantification of the in-plane damage due to earthquake loading in both CM and MI walls, using drift thresholds called Limit states or Performance Levels. In this study, three limit states, known as Immediate Occupancy (IO), Life Safety (LS), and Collapse Prevention (CP) were deemed by a Shear failure mechanism. Table 1 shows the values of the limit states obtained from MI and CM walls experimental databases gathered by different authors, together with their statistical measures, such as the median value (μ), standard deviation (σ) and the coefficient of variance (COV). These databases were used and compared between them, to derive the most adequate conditional (fragility curves) and unconditional (MAFs) failure probabilities of each structural combination, on the basis, of which database provides less conservative values.

Table 1. Limit States for MI and CM walls database.

RC MASONRY INFILL WALLS						
Authors	**IO**		**LS**		**CP**	**Data**
Cardone et al. (2015)	$\mu = 0.211\%$		$\mu = 0.616\%$		$\mu = 1.054\%$	55 walls
	σ	*COV*	σ	*COV*	σ	*COV*	
	0.09	*0.42*	*0.30*	*0.49*	*0.31*	*0.30*	
Sugano S. (2018)	$\mu = 0.219\%$		$\mu = 0.81\%$		$\mu = 1.588\%$	52 walls
	σ	*COV*	σ	*COV*	σ	*COV*	
	0.18	*0.81*	*0.54*	*0.66*	*0.96*	*0.61*	
CONFINED MASONRY WALLS						
Ruiz et al. (2009)	$\mu = 0.09\%$		$\mu = 0.31\%$		$\mu = 0.5\%$	118 walls
Sugano S. (2018)	$\mu = 0.081\%$		$\mu = 0.535\%$		$\mu = 0.927\%$	171 walls
	σ	*COV*	σ	*COV*	σ	*COV*	
	0.01	*0.88*	*0.48*	*0.90*	*0.64*	*0.69*	

7. PROBABILISTIC SEISMIC DEMAND ANALYSIS (PSDA)

The PSDA focuses on evaluating the statistics of the dynamic responses of a structure and being able to derive seismic demand fragility curves. This can be achieved with the use of the Incremental Dynamic Analysis (IDA), which is based on a series of nonlinear dynamic analysis under a multiplied scaled suite of ground motion records (Vamvatsikos, D. 2002). Thus, the classified 40 ground motions mentioned above, will be used to subject the structures under this procedure. Likewise, this process allows to registering (for certain hazard levels of interest) the Record to Record Variability (RTR). Figure 5 shows the IDA results obtained for each structural combination and each IM, either PGA or Sa (T1,5%), reaching in total 5,765 analyses. Also, in this figure, a linear power relation between the 50th percentile EDPs and IM [$\overline{EDP}$=a(IM)^b] and its associated uncertainty (RTR=$\beta_{D|IM}$) for each combination, is shown.
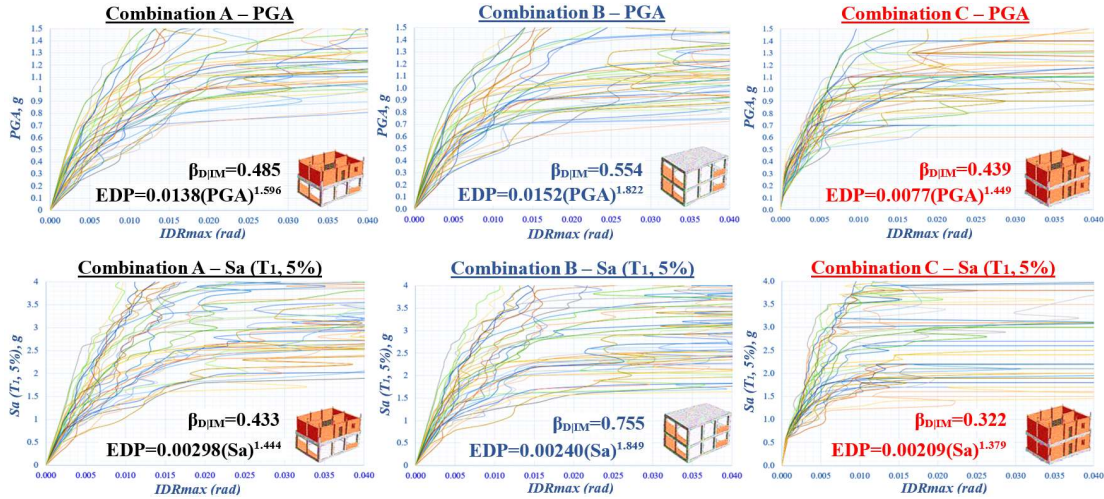

Figure 5. IDA results of each structural combination and each IM, with their equations and uncertainties.

8. PROBABILISTIC SEISMIC CAPACITY ANALYSIS (PSCA)

The PSCA relates the EDPs with damage measures (DMs) connected to the real structural deformation capacity that an element could have. Thus, the seismic damage fragility functions can be obtained. It is important to emphasize that the only way to assess the median capacity (m_c) and random uncertainties (βcr) is to compare empirical models with real experimental data, for each limit state, making use of the databases shown in Table 1. Figure 6, shows an example of the procedure carried out for the combination C and its Life Safety limit state, associated with the deformation at maximum strength (Rmax) from its backbone curve. First, the experimental over calculated capacity ratio (Rexp/Rcalc) is computed. Second, the statistics of these ratios are found through fitting them to a lognormal distribution, obtaining the aleatory uncertainty (βcr). Finally, the median capacity will be derived by multiplying the 50th percentile of the ratios to the deterministic capacities (mc^d) obtained from a static pushover analysis.
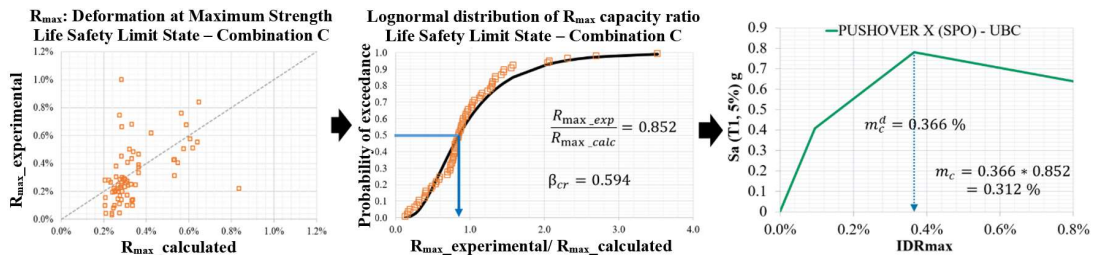

Figure 6. Procedure to determine the median capacity and structural capacity uncertainty.

9. SEISMIC DAMAGE FRAGILITY FUNCTIONS (CONDITIONAL PROBABILITY)

The seismic fragility functions or also known as fragility curves represent the failure probability of structural element exceeding a limit state conditioned to a specific earthquake ground motion. Assuming that the seismic response of structures follows a lognormal distribution, these fragility curves can be obtained through two approaches. The first related only to consider the seismic demand response uncertainties (RTR=$\beta_{D|IM}$), and the second one, with the introduction of both seismic demand and seismic structural capacity uncertainties (β_C). The latter includes both the randomness in the material properties, geometric characteristics (β_{Cr}) and the epistemic uncertainties (β_{CU}) in the modeling, design requirements and test data. These epistemic uncertainties were treated under a quality approach using predefined values suggested by FEMA P695, where a value of 0.28 was determined. Eq. (1) shows the formulation of the seismic damage fragility function and Figure 7 shows the results of this concept to each limit state (displaying its respective m_c and β_C for each combination and using both IM, i.e. PGA or Sa (T1, 5%), highlighting the existing sensitivity when using different IM in the fragility analysis.

$$F_{R_C}\left(im = x\right) = 1 - \Phi\left[\frac{\ln\left(m_C / \overline{EDP}\right)}{\sqrt{\beta_C^2 + \beta_{D|IM}^2}}\right] = \Phi\left[\frac{\ln\left[a(x)^b - m_C\right]}{\sqrt{\beta_{D|IM}^2 + \beta_C^2}}\right] = \Phi\left[\frac{\ln x - \ln\left(m_C / a\right)^{1/b}}{\frac{1}{b}\sqrt{\beta_{D|IM}^2 + \left(\beta_{Cr}^2 + \beta_{CU}^2\right)}}\right] \quad (1)$$

where, $\Phi\left[\cdot\right]$ is the standard normal probability distribution, x is any value of a ground motion (*im*), from PSDA (see Figure 5): $\overline{EDP}$ is the median EDP drift value (*a* and *b*, are regression parameters) and ($\beta_{D|IM}$) is the seismic demand uncertainty, from PSCA (see Figure 6): (m_c) is the median capacity, (βcr) is the seismic capacity aleatory uncertainty and (βcu) is the seismic capacity epistemic uncertainty.
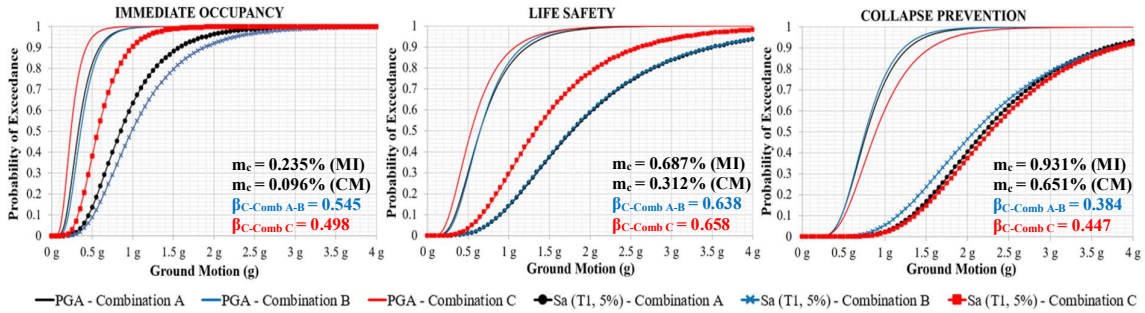

Figure 7. Seismic Damage Fragility Functions for three combinations and both IM (PGA, Sa (T$_1$,5%).

10. SEISMIC RELIABILITY ANALYSIS (SRA-UNCONDITIONAL PROBABILITY)

The SRA is based on MAF computation of exceeding a limit state of a structural element, where on this occasion it would not be conditioned to a specific value of ground motion, but on a whole intensity domain, covering all possible earthquakes that can occur in a particular area and to which the structure can be exposed. Considering again the seismic demand and structural capacity uncertainties, the unconditional failure probability can be computed by convolving the seismic damage fragility curve with the slope of the seismic hazard curve, as expressed in Eq. (2):

$$\lambda_{DM}\left(C\right) = \lambda\left(D \ge C\right) = \int_x F_{R_C}\left(x\right)\left|d\lambda_{IM}\left(x\right)\right| = k_0 \cdot \left(\frac{m_c}{a}\right)^{1/b} \exp\left[\frac{1}{2}\frac{k^2}{b^2}\left[\beta_{D|IM}^2 + \left(\beta_{Cr}^2 + \beta_{CU}^2\right)\right]\right] \quad (2)$$

where, from PSHA: k_0 and k are regression parameters, as shown in Figure 3 for PGA. It should be mentioned, that this was also done for the Sa (T$_1$, 5%). The other parameters were explained in Eq. (1).

Table 2 shows the results of failure probability of three structural combinations, highlighting whether or not they meet a desired acceptance criteria associated with the MAF of an Earthquake Design Levels. Similarly, it is shown which of the combinations presents more structural reliability, based on higher return periods to exceed a specific limit state.

Table 2. Unconditional failure probability for 3 combinations and both (IM) [PGA or Sa (T$_1$, 5%)].

Limit State	IM = PGA Failure Probabilities in terms of Return Period (RP years: 1/λ$_{DM}$) Combinations			PGA - Earthquake Design Levels (years)											
				72 years Combinations			250 years Combinations			475 years Combinations			975 years Combinations		
	A	B	C	A	B	C	A	B	C	A	B	C	A	B	C
IO	15	22	6	FAILS	FAILS	FAILS	FAILS	FAILS	FAILS	FAILS	FAILS	FAILS	FAILS	FAILS	FAILS
LS	98	117	44	PASS	PASS	FAILS	FAILS	FAILS	FAILS	FAILS	FAILS	FAILS	FAILS	FAILS	FAILS
CP	286	285	359	PASS	PASS	PASS	PASS	PASS	PASS	FAILS	FAILS	FAILS	FAILS	FAILS	FAILS
	IM = Sa(T$_1$, 5%)			Sa(T$_1$, 5%) - Earthquake Design Levels (years)											
IO	12	15	7	FAILS	FAILS	FAILS	FAILS	FAILS	FAILS	FAILS	FAILS	FAILS	FAILS	FAILS	FAILS
LS	73	67	54	PASS	FAILS	FAILS	FAILS	FAILS	FAILS	FAILS	FAILS	FAILS	FAILS	FAILS	FAILS
CP	210	141	413	PASS	PASS	PASS	FAILS	FAILS	PASS	FAILS	FAILS	FAILS	FAILS	FAILS	FAILS

= More Reliable   = Less Reliable   PASS means Failure Probability (in terms of RP) higher than RP of Eathquake Design Level

11. CONCLUSIONS

The investigation resulted in the following main conclusions:
- When the aleatory and epistemic uncertainties of both seismic demand and structural capacity are not taken into account, the real fragility of the structure can be overestimated.
- According to Seismic Damage Fragility Curves, for the Immediate Occupancy (IO) and Life Safety (LS) limit states, the combination C presents the higher fragility than the others. However, in Collapse Prevention (CP) limit state, less fragility is observed.
- For IO and LS limit states, the Combination B has the highest structural reliability for PGA and Combination C has the lowest seismic performance in both (IM). For CP limit state, the Combination C has the highest structural reliability for both (IM)
- None of the combinations managed to meet the acceptable MAFs at the less frequent seismic hazard levels of 475 and 975 years of Return Period (RP), in any limit states.

REFERENCES

Cardone, D., and Perrone, G., 2015, Earthquakes and Structures, Vol. 9, No. 1, 257-279.
FEMA P695, 2009, Washington, D.C.
Lu, D.G., Yu, X.H., and Jia, M.M., 2012, Harbin Institute of Technology, Harbin, 150090, China.
Mostafaei, H., and Kabeyasawa, T., 2004, Bull. Earthq. Res. Inst., Earthquake Spectra 24, 701–723.
Ruiz-García, J., and Negrete, M., 2009, J. Earthq. Eng., 13, 520-539.
Saito, T., 2004, Structural Response Analysis 3D (STERA 3D v.9.6 in 2018), Technical Manual, Japan.
Sugano, S., 2018, Lecture notes on Masonry Structures II, IISEE/BRI (2017-2018).
Vamvatsikos, D., and Cornell, C.A., 2002, Earthq. Engineering & Structural Dynamics, 31, 491–514.